Original Research

Spatial and Temporal Heterogeneity of Human-Air-Ground Coupling Relationships at Fine Scale

Huaizhen Peng[1,2], Huachao Lou[3], Ying Yang[4], Qingying He[1,2], Yifan Liu[1,2], Enqing Chen[5], Maomao Zhang[6]*

[1]College of Landscape Architecture, Central South University of Forestry Technology, Changsha 410004, China
[2]Engineering Technology Research Centre of Big Data for Landscape Resources in Nature Protected Areas of Hunan Province, Changsha 410004, China
[3]Management Committee of Hangzhou Campus of Zhejiang Normal University, Hangzhou, 321004, China
[4]General Design and Research Institute, China Construction Fifth Engineering Bureau Co
[5]School of Education and Foreign Languages, Wuhan Donghu University, Wuhan 430212, China
[6]College of Public Administration, Huazhong University of Science and Technology, Wuhan 430079, China

Abstract

The study of the spatial and temporal evolution of annual mean $PM_{2.5}$ concentration and population exposure risk in Hunan Province can further analyze the influence of the landscape pattern index on the changes in annual mean $PM_{2.5}$ concentration and population exposure risk. The spatial and temporal evolution of the coupling relationship between people, air, and land at a fine scale and its spatial heterogeneity were investigated by the population exposure risk model, the moving window method, the spatial auto correlation model, and correlation analysis. The results show that: (1) from 2000 to 2020, the annual average $PM_{2.5}$ concentration in Hunan Province showed a slow increase and then a significant decrease, and its spatial distribution was high in the northeast and low in the southwest. (2) From 2000 to 2016, the average proportion of the population exposed to high annual average $PM_{2.5}$ concentrations (>45 μg/m³) in Hunan Province reached 74.24%, and from 2016 to 2020, the proportion of the population exposed to low annual average $PM_{2.5}$ concentrations (<35 μg/m³) increased year by year. In 2020, there were regions with annual average concentrations of 15-25 μg/m³, and the regional concentrations were all less than 45 μg/m³. The spatial distribution is dominated by low-risk areas, with an overall scattered distribution, and high-risk areas are concentrated in the Chang - Zhu - Tan urban agglomeration. (3) Cultivated land and forested land, as the main land types, have relatively obvious characteristics of changes in dynamics and attitudes; water bodies and impervious surfaces are second; cultivated land has a high degree of patch aggregation, high edge density and low fragmentation, which increases the risk of annual average $PM_{2.5}$ concentration and population exposure; forested land has a high degree of patch aggregation, low edge density and low fragmentation, which is conducive to reducing the risk of annual average $PM_{2.5}$ concentration and population exposure; and water bodies

*e-mail: star_mzhang@mails.ccnu.edu.cn

and impervious surfaces have a high degree of aggregation, low edge density, and low fragmentation, which is conducive to reducing the risk of annual average $PM_{2.5}$ concentration and population exposure. The higher the degree of aggregation, the higher the edge density, the more complex the degree of fragmentation of water bodies and impervious surfaces, and the higher the risk of annual average $PM_{2.5}$ concentration and population exposure. The results of this study can provide a theoretical basis for mitigating air pollution, improving the human environment, optimizing the landscape pattern, and promoting ecologically sustainable development.

Introduction

Accompanied by the acceleration of urbanization, the problem of air pollution has become increasingly prominent [1, 2]. Population expansion, urban infrastructure construction, and industrial development have led to increased emissions of pollutant gases and rising pressure on the ecological environment. The contradiction between the people's growing demand for a beautiful ecological environment and the continuous deterioration of the ecological environment is prominent [3]. Urban and regional air pollution, represented by fine particulate matter ($PM_{2.5}$), not only poses a great threat to public health but also damages the ecological environment, thus hindering the sustainable development of cities [4]. Therefore, it is important to study the temporal dynamic pattern of $PM_{2.5}$ concentration in different regions, its spatial pattern distribution, and its interrelationship with various influencing factors in order to control air pollution, optimize the construction of the ecological environment, improve the human habitat, and build a healthy city.

At present, the study of the spatial and temporal distribution pattern of $PM_{2.5}$ concentration and the exploration of its formation mechanism and influencing factors is one of the hotspots of atmospheric environment research [5]. Scholars at home and abroad on air pollution ($PM_{2.5}$) research are mainly focused on source analysis [6], spatial and temporal evolution [7, 8], driving mechanisms [9], scenario simulation [10], and health evaluation [11, 12], and its influencing factors include meteorological factors, population density, land use, road traffic, topographic changes, and sources of pollution. They are gradually paying attention to the influence of landscape patterns on $PM_{2.5}$ concentration. In terms of the spatial and temporal distribution and evolution of $PM_{2.5}$, the study presents the diversification of data sources [13], the refinement of scales [14], and the diversification of methods [15]. Its different scales include national scales [16], regional scales [17], provincial scales [18], urban scales [19], etc. Specifically, in terms of the influence of population factors on $PM_{2.5}$ concentration, the study focuses on population exposure risk to pollution sources, evolutionary pathways, and policy formulation [20], with population density [21] and population weighting [22] as the two main methods,

and mostly using administrative districts as the research unit. Such studies are unable to characterize the severity of population exposure risk within refined spatial units [23], and there are some limitations in exploring the spatial heterogeneity of $PM_{2.5}$ population exposure risk in depth. In contrast, the population exposure relative risk model can effectively quantify the degree of risk of population exposure to $PM_{2.5}$ concentrations within a spatial unit [24]. It can more finely and accurately analyze the interrelationships between demographic factors and $PM_{2.5}$ concentrations in a spatial unit. For example, Chen [25] compared air quality concentrations and population spatial distribution, proposed a population air pollution exposure assessment model, and then quantified the degree of population air pollution exposure within a spatial unit. Singh [26] differentiated the risk of population air pollution exposure on a fine scale by superimposing atmospheric pollutants and the spatial distribution of the population on the internal grid of the spatial unit, and some scholars have further discussed the impacts of landscape pattern factors on $PM_{2.5}$ concentrations on the spatial unit from a geographic point of view. Some scholars further discussed the influence of landscape pattern factors on $PM_{2.5}$ concentration from a geographic perspective, e.g., LIM A [27] found that $PM_{2.5}$ concentration was positively proportional to the area of patches and the number of patches and inversely proportional to the average perimeter-area ratio and the average Euclidean distance. SHARMA D [28] and GHESHLAGHPOOR S [29] mainly investigated the relationship between particulate pollutant data and urban land use/cover characteristics, and the correlation between air pollutant distribution and concentration was found to be different from the spatial pattern of land use. MENGISTE B.M [30] found that the higher the degree of landscape dominance and the stronger the connectivity of patches, the more capable of reducing $PM_{2.5}$ concentration through multiple linear regression analysis it is. McCarty [31] found that changes in landscape patterns would affect the spatial distribution of $PM_{2.5}$ and increase the risk of exposure for the population by combining the correlation between the landscape pattern of the urban landscape and air quality analysis. It can be seen that the above studies focus more on the influence of single-factor changes on the spatial and temporal distribution

and evolution of PM$_{2.5}$ concentration. In correlation analysis, only population and landscape patterns are analyzed independently on the trend of spatial and temporal evolution of PM$_{2.5}$ concentration, which does not fully reveal the spatial heterogeneity and mutual interference among factors and lacks the differences in the influence of multiple factors on PM$_{2.5}$ at a fine scale. Therefore, it is particularly important to explore the coupling relationship between population, landscape pattern, and air pollution (PM$_{2.5}$) in spatial distribution to further quantitatively analyze the spatial and temporal evolution characteristics of 'Human-Air-Ground' and its spatial heterogeneity at fine scales and to provide entry points and breakthroughs for the sustainable development of regional ecological environments.

Against this background, the author takes Hunan Province as the study area uses PM$_{2.5}$ concentration data, population distribution data, and six-phase land-use type data from 2000 to 2020, and takes a 5 km × 5 km grid as the study unit. It introduces the relative risk model, the spatial auto correlation model, and the correlation coefficient method of population exposure to match population distribution at the scale of the refinement grid and the administrative district. By matching the population distribution, PM$_{2.5}$ concentration, and landscape pattern indices at the scale of refined grids and administrative districts, we reveal the spatial and

temporal evolution characteristics of the coupling relationship between 'Human-Air-Ground' and its spatial heterogeneity. In this paper, the following three aspects of the coupling relationship are investigated: ① Identify the characteristics of the spatial and temporal evolution of PM$_{2.5}$ concentration in the study area under long time series; ② Explore the spatial and temporal evolution of PM$_{2.5}$ concentration and population exposure risk in the study area, and accurately identify the degree of PM$_{2.5}$ population exposure risk; ③ Reveal the spatial and temporal evolution characteristics of the coupling relationship between 'Human-Air-Ground' and its spatial heterogeneity in the study area. The study results can provide a theoretical basis for mitigating atmospheric pollution, improving the human environment, optimizing the landscape pattern, and promoting ecologically sustainable development.

Materials and Methods

Study Area

Hunan Province is located in the middle and lower reaches of the Yangtze River, at 24°39′N-30°08′N, 108°47′E-114°15′E (Fig. 1), with 13 prefectural-level cities, 1 autonomous prefecture, and 122 districts and
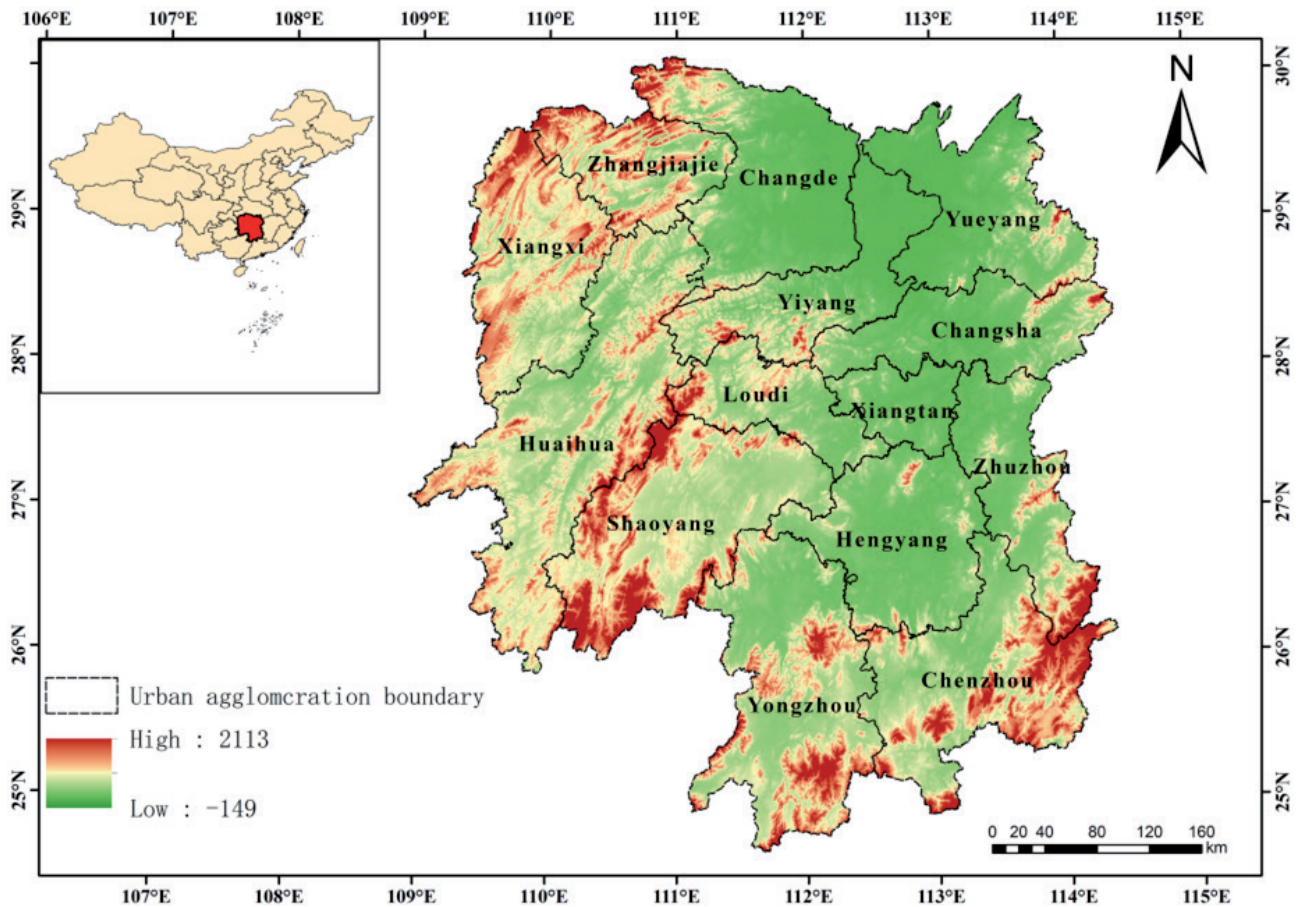

Fig. 1. Study area extent and elevation.

counties, covering an area of 211,800 km². The terrain is predominantly mountainous and hilly, with interspersed plains, basins, rivers, and lakes, and decreases in a gradient from west to east. Most of the study area has a subtropical monsoon climate, with an average annual temperature of 16-18 °C and an average annual rainfall of 1,200-1,700 mm. By the end of 2023, the resident population of Hunan Province will be 65.68 million, a year-on-year decrease of 0.5%; the gross domestic product (GDP) will be 50,012.09 billion yuan, a year-on-year increase of 4.6%; and the gross regional product (GDP) per capita will be 75,938 yuan, a year-on-year increase of 5.0%. The achievements in economic construction have also brought great challenges to air quality, the most obvious phenomenon of which is the frequent occurrence of haze weather, with $PM_{2.5}$-based haze pollution problems being more prominent. The landscape pattern of the region is characterized by greater spatial heterogeneity and evolution due to the long-term combined effects of anthropogenic activities and social factors.

Data Source and Processing

The study's main data includes digital elevation (DEM), administrative boundaries of Hunan Province, annual average concentration of $PM_{2.5}$, population distribution, and land use types. Considering the need to maintain the consistency of the relevant data time period, every four years was chosen as the interval period, with a total of six data periods in 2000, 2004, 2008, 2012, 2016, and 2020. ArcGIS software was used to crop and extract the study area data according to the administrative boundaries and reclassify the land use types into cropland, forest land, shrubland, grassland, water bodies, bare land, and impervious surface. Due to the differences in the data resolution, the spatial resolution was resampled to 300 m to ensure spatial and temporal matching on a uniform coordinate system. The data sources and processing are shown in Table 1.

Methods

Population Exposure Risk

In order to scientifically quantify the risk of population exposure to $PM_{2.5}$ pollution, this paper introduces the relative risk evaluation model of population air pollution exposure [32]. This is mainly to multiply the proportion of the population in each cell of the study area to the population of the whole area with the concentration of $PM_{2.5}$ in the cell to obtain the contribution value of the cell to the risk of population exposure to $PM_{2.5}$, and then add the contribution value of each cell of the study area to obtain the population-weighted concentration exposure index of $PM_{2.5}$ in the study area. The contribution of each cell in the study area was then summed to obtain the population-weighted $PM_{2.5}$ exposure indicator for the area. The specific calculation formula is as follows:

$$R_i = \frac{P_i \times C_i}{\sum_{i=1}^{n}\left(P_i \times \frac{C_i}{n}\right)} \tag{1}$$

Where: i - grid number; R_i - risk of population exposure to $PM_{2.5}$ for the grid; P_i - number of people in the grid; C_i - $PM_{2.5}$ concentration value within the grid; n - total number of grids.

Moving Window Method

In order to comprehensively reflect the spatial distribution characteristics of landscape patterns, with reference to previous studies [33, 34], landscape pattern indices, such as aggregation index (AI), the average area of patches (AREA_MN), patch density (PD), edge density (ED), shape index (LSI), and contagion index (CONTAG), as well as the proportion of patches in the landscape area (PLAND), were selected to characterize the landscape's connectivity, degree of fragmentation, structure, shape, and compositional characteristics. Since the landscape pattern is scale-dependent, choosing

Table. 1. Data sources and processing.

| Type	Source	Description	Accuracy	Processing method
Digital Elevation Model	Geospatial data cloud	Elevation, slope, and direction of slope	30m×30m	Projection, inlay, cutting
National Administrative Boundary	Resources and Environmental Science Data Center	Vector data on administrative boundaries of provinces, cities, and counties nationwide	—	Projection, consolidation
$PM_{2.5}$ annual average concentration	National Earth System Science Data Center	High-resolution, high-quality, year-on-year, month-on-month, and day-on-day $PM_{2.5}$ data for China, 2000-2022	1 km	Projection, cropping
Population Distribution	World pop dataset	Data on the spatialization of population in China, 2000-2020	1 km	Projection, cropping
Land use type	China land cover dataset	Year-by-year landscape type data for China, 1985-2020	30m×30m	Projection, cropping
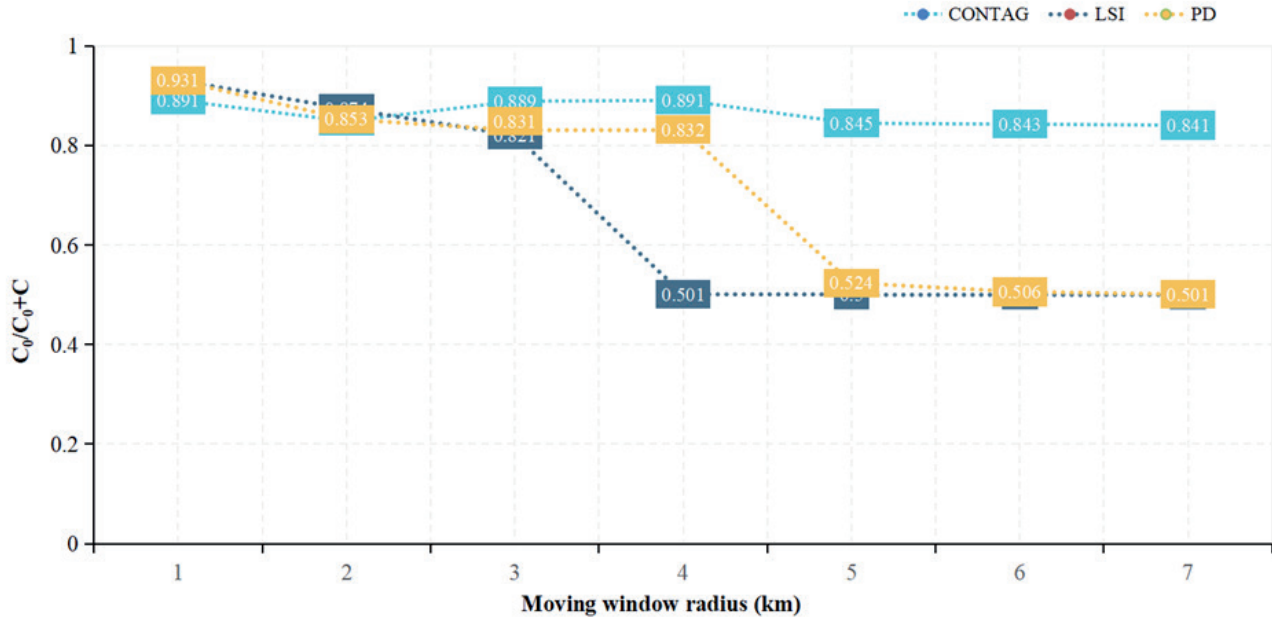
Fig. 2. Trends in the spatial variability of landscape pattern indices.

the appropriate scale can more accurately reflect the real situation of the landscape pattern; therefore, the window radius (km) was set to 1, 2, 3, 4, 5, 6, and 7 using Fragstats software. The semi-variance function in geostatistics was used to determine the optimal scale for the moving window. The ratio of the nugget value to the abutment value in the semi-variance function (nugget-base ratio) reflects the degree of spatial variability, and the smaller its value is, the more obvious the spatial autocorrelation is and the more stable the scale is. The optimal analysis scale is the window radius when the patch-to-basal ratio reaches relative stability [35, 36]. Under the continuous scale, the spreading index (CONTAG), patch density (PD), and shape index (LSI) were selected as the calculation objects, and sample strips were set up for sampling [37]. It was finally determined that the landscape pattern index tended to be stabilized at 5 km (Fig. 2), which indicated that this scale could better reflect the spatial heterogeneity of the landscape pattern.

Spatial Autocorrelation

Global spatial autocorrelation analysis was used to measure the agglomeration between spatial units and neighboring units throughout the study area, and the global Moran's index was used to determine whether $PM_{2.5}$ concentrations were spatially autocorrelated. The value of the global Moran index ranges from [-1,1], which is greater than 0 to indicate that there is a positive spatial correlation between $PM_{2.5}$ concentration and its influencing factors, less than 0 to indicate that there is a negative spatial correlation, and equal to 0 to indicate that there is no spatial autocorrelation between the regions. Local spatial autocorrelation analysis is used

to explore the degree of adjacent spatial correlation, detect the location of outliers or clusters, and determine the clustering of spatial units (districts and counties) of annual average $PM_{2.5}$ concentrations based on the local Moran index [38]. The global Moran index (I_G) and local Moran index (I_L) are commonly used, and their expressions are as follows:

$$I_G = \frac{n \sum_{i=1}^{n} \sum_{j=1}^{n} w_{ij}(x_i - \bar{x})(x_j - \bar{x})}{S^2 \sum_{i=1}^{n} \sum_{j \neq 1}^{n} w_{ij}}, \quad (i \neq j) \tag{2}$$

$$S^2 = \frac{1}{n} \sum_{i=1}^{n} (x_i - \bar{x}) \tag{3}$$

$$\bar{x} = \frac{1}{n} \sum_{i=1}^{n} x_i \tag{4}$$

$$I_L = \frac{(x_i - \bar{x}) \sum_{j=1}^{n} w_{ij}(x_j - \bar{x})}{S^2}, (i \neq j) \tag{5}$$

Where: n - total number of grids; S^2 - variance of $PM_{2.5}$ concentration of all grids; x_i and x_j - $PM_{2.5}$ concentration of the ith and jth grids; $\bar{x}$ - mean of all grid attributes; w_{ij} - spatial weights.

Land Use Dynamics

Land use dynamic attitude is the area ratio before and after the change of a certain type of land use type within a certain time range in the study area, which can reflect the change of land use in type, quantity, speed, and ecological quality in different periods [39]. In the paper, the land use dynamic index model was applied to dynamically analyze the changes in type, quantity, and speed in different periods in the study area. Its single
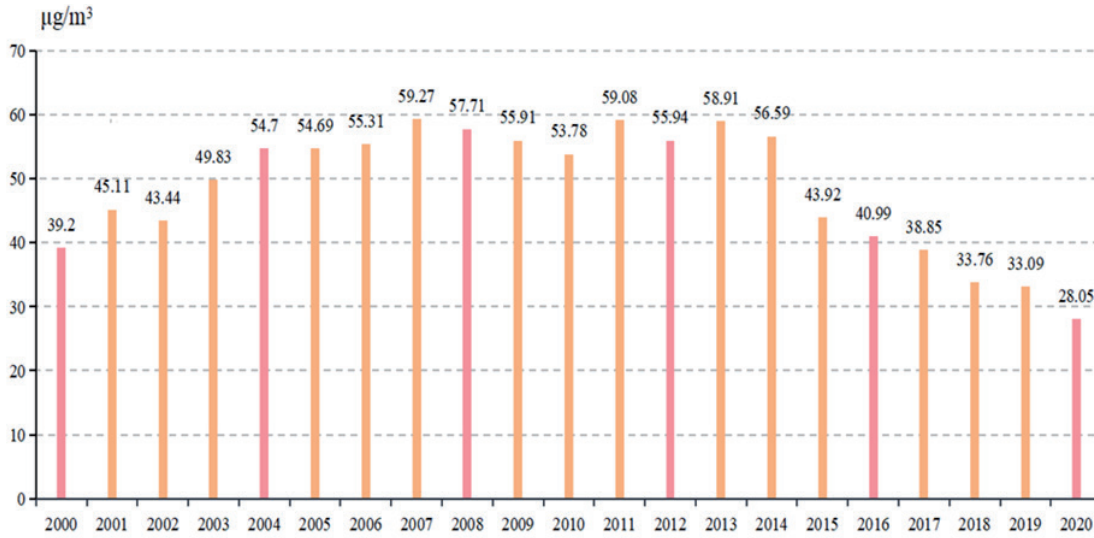
Fig. 3. Trend of annual average PM$_{2.5}$ concentration in Hunan Province.

land use dynamics can express the change of a certain land use type within a certain time range in a specific area, while the comprehensive land use dynamics can reflect the annual rate of change of all the land uses in the whole area. The specific model formula is as follows [40]:

Single land-use attitudes

$$D_s = \frac{U_b - U_a}{U_a} \times T^{-1} \times 100\% \qquad (6)$$

Integrated land-use dynamics

$$D_c = \left(\frac{\sum_{i,j=1}^{n} \Delta U_{ij}}{2 \sum_{i=1}^{n} U_i} \right) \times T^{-1} \times 100\%, (i \neq j) \qquad (7)$$

Where: U_a and U_b - area of a land-use type (km^2) at the beginning and end of the study period; U_i - area of a land-use type of type i (km^2), ΔU_{ij} - absolute value of the area of land-use type i converted to type i during the study period ($i \neq j$); T - length of the study (years).

Results and Discussion

Characteristics of the Spatial and Temporal Evolution of PM$_{2.5}$

Characterization of Temporal Heterogeneity

Analyzing the trend change of annual average PM$_{2.5}$ concentration in Hunan Province from 2000 to 2020, it is found that its annual average change has a certain volatility, and the whole is characterized by a slow increase and then a significant decline, reaching a maximum of 59.27 μg/m^3 in 2007 and falling to a minimum of 28.05 μg/m^3 in 2020. As can be seen in Fig. 3: PM$_{2.5}$ concentration increased slowly from the initial

39.2 μg/m^3 to 58.91 μg/m^3 in 2000-2013, with an average annual growth rate of 3.59%; PM$_{2.5}$ concentration decreased significantly from the initial 58.91 μg/m^3 to 28.05 μg/m^3 gradually in 2013-2020, with an average annual decrease rate of 13.7%. 55% of the years had annual average PM$_{2.5}$ concentrations above 50 μg/m^3, and up to 85% of the years had annual average PM$_{2.5}$ concentrations exceeding the standard value of 35 μg/m^3. Although it dropped to below the maximum limit value (35 μg/m^3), it was stipulated in the Ambient Air Quality Standard after 2018 [41] that it was still nearly twice as high as the international standard value (15 μg/m^3) [42-43]. This indicates that the pollution level is still relatively high in most parts of Hunan Province, and the pollution situation cannot be ignored.

Characterization of Spatial Heterogeneity

In order to reveal the characteristics of changes in the spatial distribution of annual mean PM$_{2.5}$ concentration, it was divided into seven intervals of (15, 25), (25, 35), (35, 45), (45, 55), (55, 65), (65, 75), and (75, +∞) in conjunction with the international standard limit values (annual mean concentration of 15, 25, and 35 μg/m^3), with every 4 years as the interval period (Fig. 4). It can be seen that: (1) The overall spatial distribution was high in the northeast and low in the southwest. The spatial distribution patterns were generally similar in 2000, 2004, and 2008, with the region-wide annual mean concentration continuing to increase, the northeast region expanding significantly, and the southwest region relatively slow, especially in 2008, when the region-wide annual mean concentration reached more than 45 μg/m^3. In 2012, 2016, and 2020, the region-wide annual mean concentration continued to decline, and the northeast region is significantly down compared with the southwest region, which is relatively slower, especially in 2020. The annual average concentration of
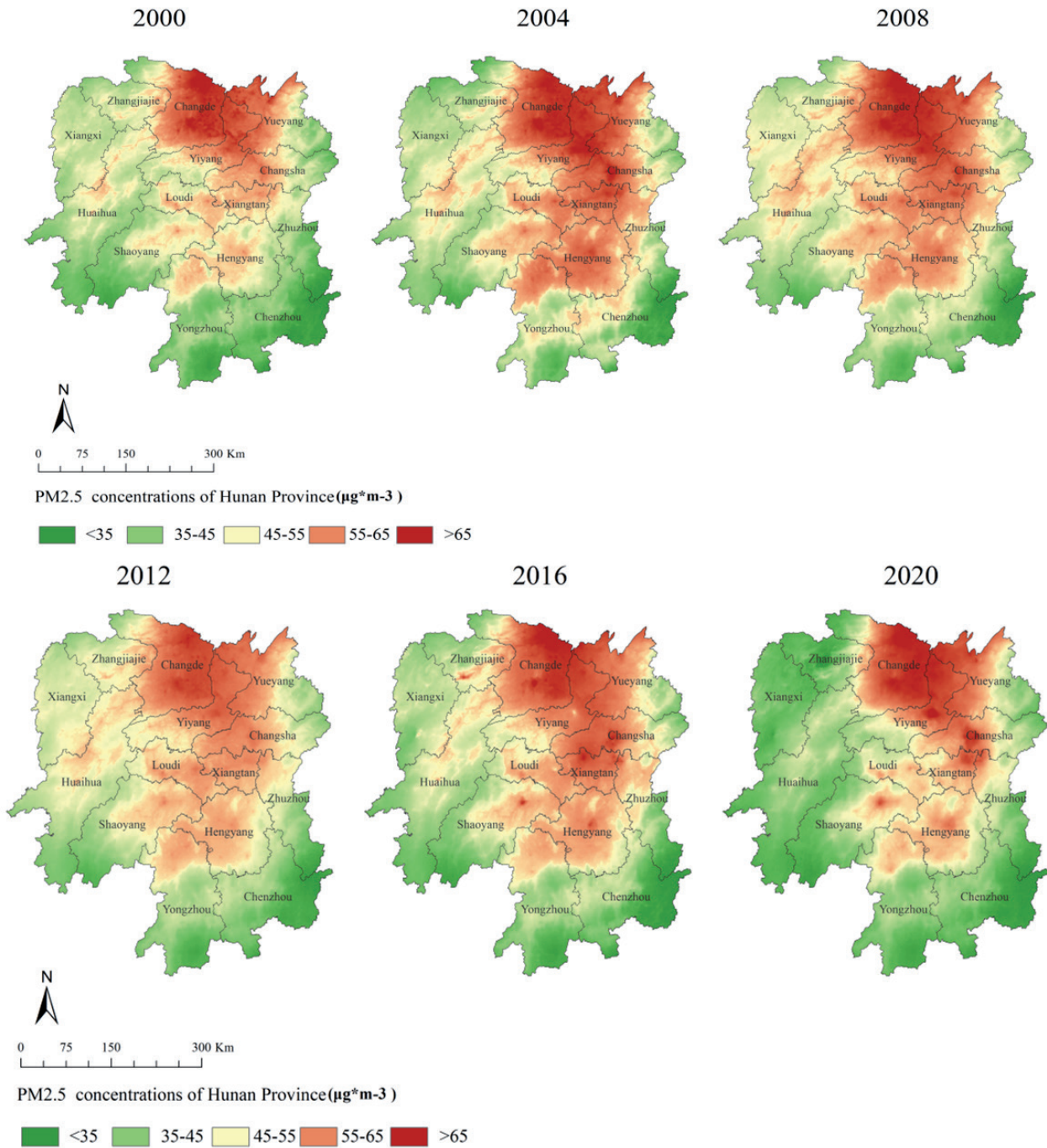
Fig. 4. Changes in the spatial distribution of annual average PM$_{2.5}$ concentration in Hunan Province from 2000 to 2020.

the whole region reached 35 µg/m³ or less and is below the maximum limit of domestic air quality standards. However, there is still a gap from the target value. (2) There are obvious differences in the local spatial distribution; for example, in 2004, 2008, and 2012, the high-value areas (>45 µg/m³) were mainly distributed in Changsha, Xiangtan, Zhuzhou, Changde, Yueyang, and Yiyang; in 2016 and 2020, the areas with annual average concentrations of less than 35 µg/m³ in this urban agglomeration have increased significantly, and in particular, in 2020, the annual average concentration in the whole area will reach below 35 µg/m³.

Geoda software carried out the global spatial autocorrelation test of annual mean PM$_{2.5}$ concentration in Hunan Province, and the global Moran's index was used to determine whether the annual mean concentration of different grids had spatial autocorrelation [44]. The Moran's index remained stable from 2000 to 2020, and all of them were over 0.8 (Table 2), which showed a significant positive autocorrelation in spatial distribution, indicating that the spatial distribution had agglomeration characteristics.

In order to further explore the spatial distribution characteristics of the annual average PM$_{2.5}$

Table. 2. Global spatial autocorrelation analysis of annual average PM$_{2.5}$ concentration in Hunan province.

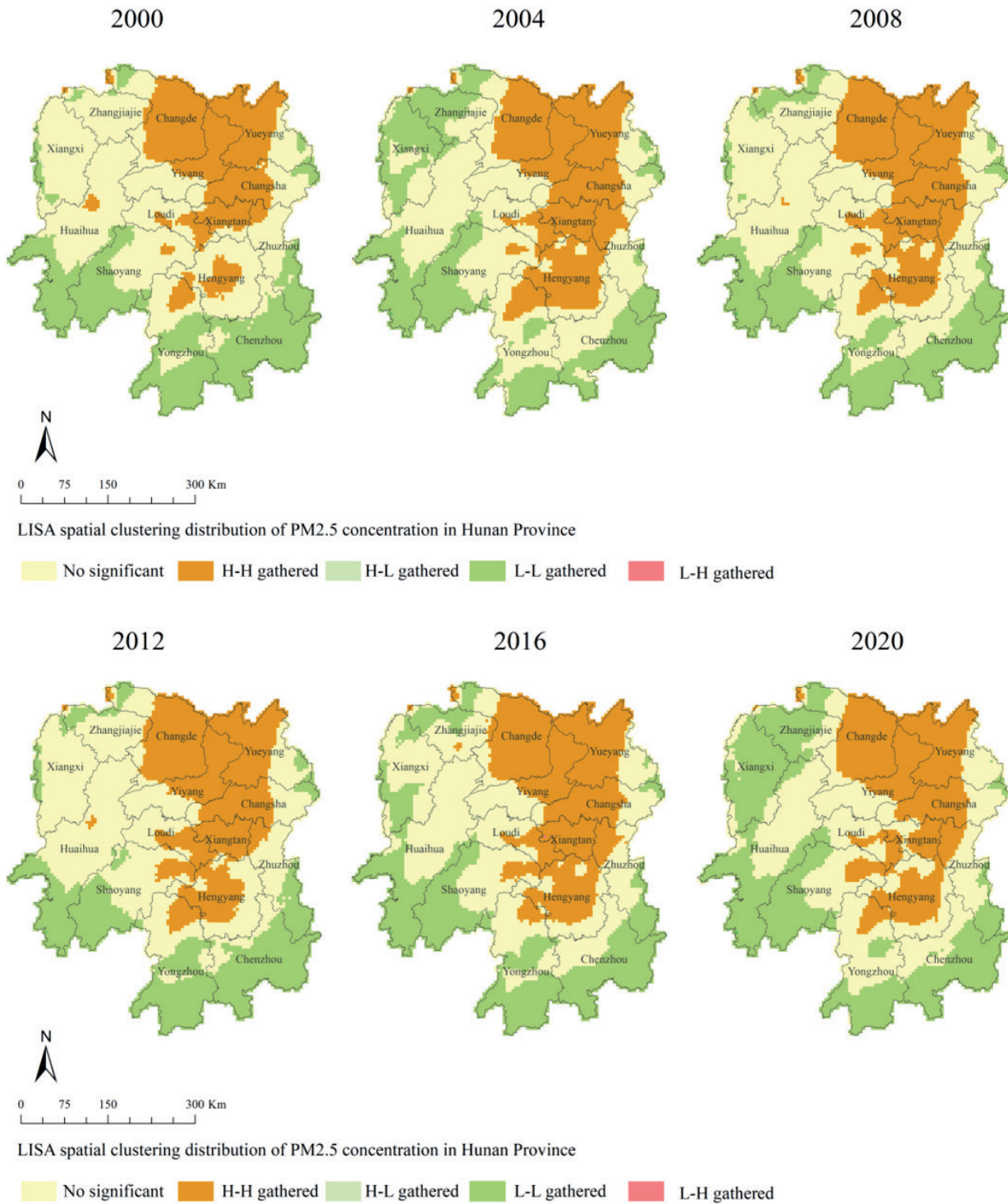| Parameters	2000	2004	2008	2012	2016	2020
Moran's I	0.834	0.810	0.831	0.841	0.836	0.827
P-value	0.001	0.001	0.001	0.001	0.001	0.001
Z-value	14.8634	14.5478	14.8182	14.8845	14.8449	14.9690

Fig. 5. LISA spatial clustering distribution of PM$_{2.5}$ concentration in Hunan Province from 2000 to 2020.
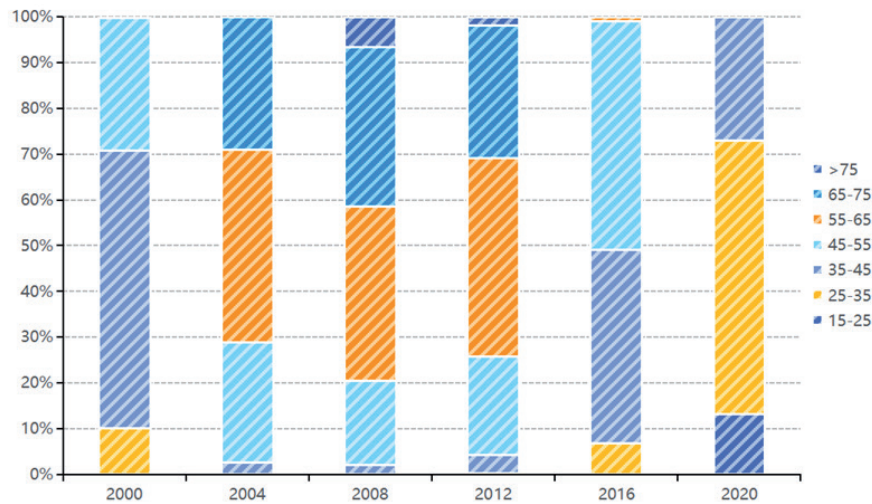
Fig. 6. Percentage of population exposure to annual average $PM_{2.5}$ concentration by zone in Hunan Province in a typical year.

concentration, the local spatial autocorrelation test was carried out with the grid as the spatial unit. According to the degree of aggregation of high or low values in each grid, it is categorized into four spatial correlation patterns: high - high aggregation area, low - low aggregation area, high - low aggregation area, and low - high aggregation area [45]. As shown in Fig. 5, local spatial aggregation characteristics are obvious; the high - high aggregation area is mainly concentrated in all or part of the districts and counties of Changsha, Xiangtan, Zhuzhou, Changde, Yueyang, Yiyang, and Hengyang, which are located in the center of economic development of urban agglomerations, with flat terrain and urban concentration, active human activities, and aggregation of $PM_{2.5}$ air pollutants. The low - low aggregation zone is mainly located in all or part of Yongzhou, Chenzhou, Huaihua, and Shaoyang, which are relatively socio-economically backward, with mountainous hills, high vegetation cover, and superior ecological environments conducive to the deposition and absorption of $PM_{2.5}$ pollutants.

Characterization of the Spatial and Temporal Evolution of the Risk of $PM_{2.5}$ Population Exposure

Temporal Heterogeneity

The statistics and visualization of the percentage of the population exposed to $PM_{2.5}$'s annual average concentration in each zone from 2000 to 2020 are shown in Fig. 6. (1) The mean percentage of the population exposed to high-concentration zones (>45 μg/m³) amounted to 74.24% in 2000-2016, while the mean percentage of the population exposed to more than 35 ug/m³ was as high as 96.5%. (2) Between 2016 and 2020, the proportion of the population in areas exposed to annual average $PM_{2.5}$ concentrations (<35 μg/m³) increased year by year, from 6.86% to 73.02%; among them, in 2020, there was an area where the

annual average $PM_{2.5}$ concentration was located in the range of 15-25 μg/m³, with a proportion of 13.2% of the population, and there were no areas with more than 45 μg/m³.

Spatial Heterogeneity

In order to scientifically quantify the degree of risk of population exposure to $PM_{2.5}$ concentration in a spatial cell (grid), systematic sampling was conducted according to a 5 km × 5 km grid with equal distances to extract the annual average $PM_{2.5}$ concentration and the number of people at the sample points. The degree of risk of population exposure to $PM_{2.5}$ concentration in a spatial cell was measured using the formula for population exposure risk in the previous section (Section 1.3). Combined with the existing literature [46, 47], the population exposure risk is categorized into six levels: low risk (0, 1), lower risk (1, 2), medium risk (2, 3), higher risk (3, 4), high risk (4, 5), and very high risk (5, +∞). As can be seen from Fig. 7, the spatial distribution of the risk level of $PM_{2.5}$ population exposure in Hunan Province from 2000 to 2020 is dominated by low risk, accounting for more than 70% of the total area, which is mainly distributed in the marginal cities and districts and counties, while the high-risk areas are mainly concentrated in the central urban agglomeration of Chang - Zhu - Tan. The rest is distributed in the form of a scattering point.

Using Geoda software to conduct a global spatial autocorrelation test of $PM_{2.5}$ population exposure risk in Hunan Province, Moran's index remained stable and close to 0.5 from 2000 to 2020 (Table 3). This indicates a positive autocorrelation in the spatial distribution, suggesting that the spatial distribution of $PM_{2.5}$ population exposure risk exhibits a clustering characteristic.

Analyzing the local spatial autocorrelation test of $PM_{2.5}$ population exposure risk in Hunan Province

2000   2004   2008

PM2.5 Population Exposure Risk Levels(grade 1 = lowest, grade 5 = highest).

1   2   3   4   5

2012   2016   2020

PM2.5 Population Exposure Risk Levels(grade 1 = lowest, grade 5 = highest).
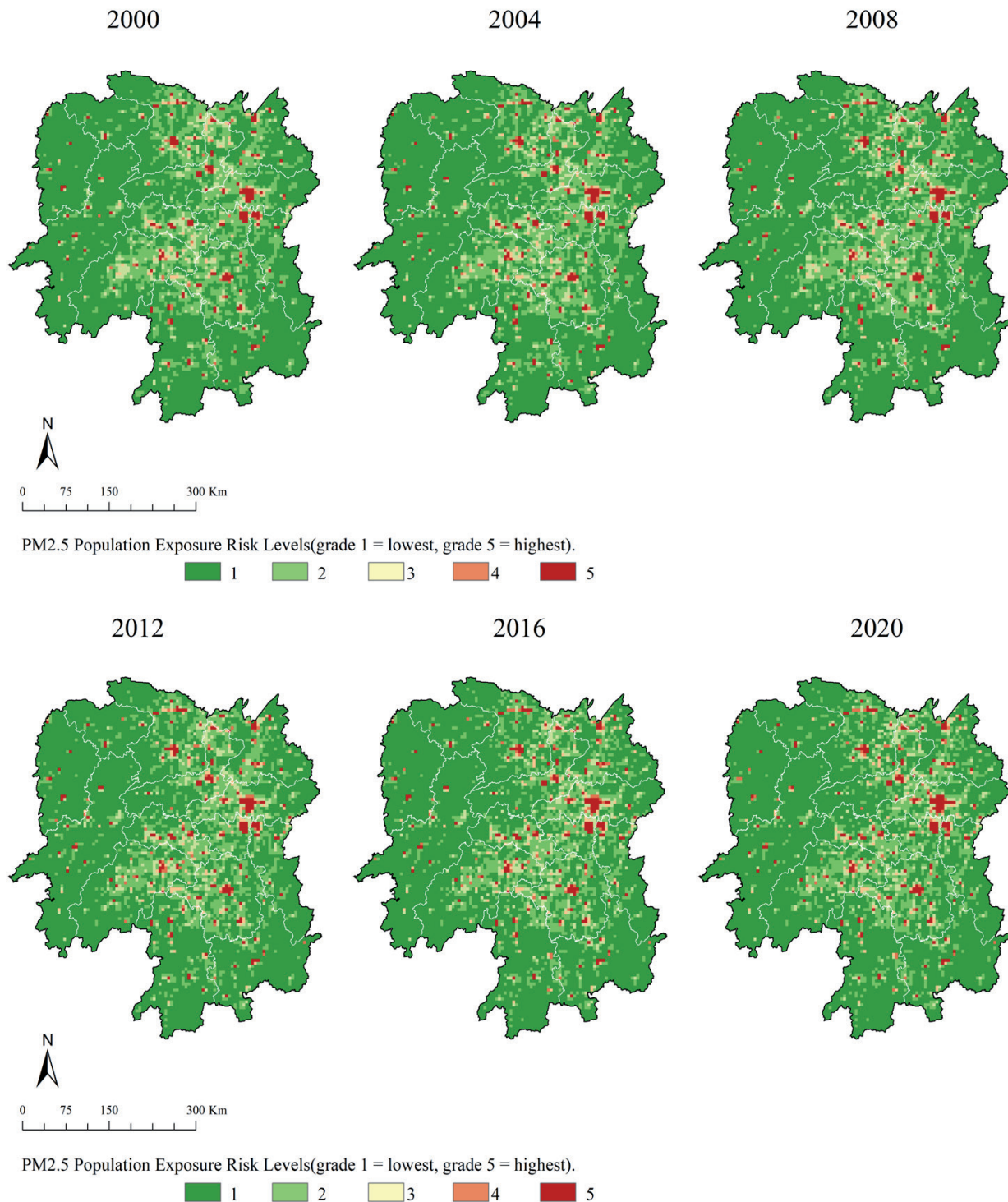
1   2   3   4   5

Fig. 7. Change in the spatial distribution of PM$_{2.5}$ population exposure risk level in Hunan Province from 2000 to 2020.

from 2000 to 2020 (Fig. 8), we found that the spatial correlation pattern is the same as the spatial clustering characteristics of PM$_{2.5}$ annual average concentration (Section 2.1.2). The high - high aggregation area is distributed in a cluster shape, and the scope changes are small, mainly concentrated in the core area of Chang - Zhu - Tan city, which is fundamentally due to the urbanization and industrialization development triggered by the population concentration leading to the growth of

PM$_{2.5}$ emissions, and the high-risk area is concentrated in the city center, which exposes the population to the high-concentration range for a long period of time. The low - low concentration zones are mainly located in Yongzhou, Chenzhou, Huaihua, and Shaoyang, which are related to their hilly and mountainous location, high vegetation cover, small population size, slow industrialization, low socio-economic energy consumption, and low pollution emissions.

Table. 3. Global spatial autocorrelation analysis of PM$_{2.5}$ population exposure risk in Hunan province.

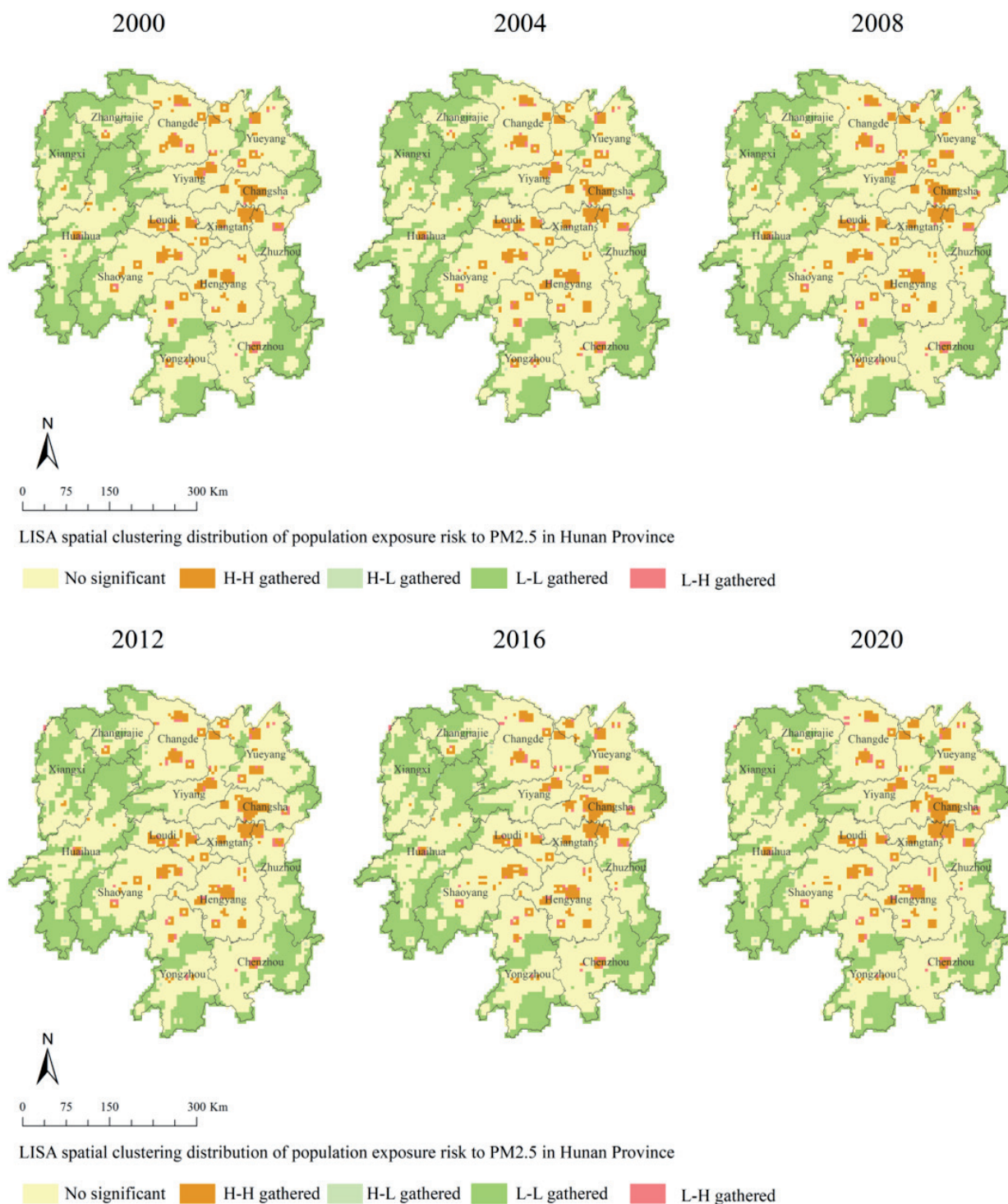| Parameters	2000	2004	2008	2012	2016	2020
Moran's I	0.493	0.497	0.495	0.494	0.496	0.496
P-value	0.001	0.001	0.001	0.001	0.001	0.001
Z-value	9.9563	10.0887	10.1023	10.1381	10.2414	10.3169

Fig. 8. LISA spatial clustering distribution of population exposure risk to PM$_{2.5}$ in Hunan Province from 2000 to 2020.

Table. 4. Area of each landscape type in Hunan Province in a typical year from 2000 to 2020 (km^2).

	2000	2004	2008	2012	2016	2020
Cropland	68360.28	69678.77	71928.57	71998.09	71964.43	71490.33
Forest	135576.98	134219.27	131734.65	131192.06	130411.89	130813.31
Shrub	242.17	209.73	149.78	96.45	68.57	61.19
Grassland	82.59	67.79	62.36	67.88	65.20	57.58
Water	5067.41	4871.51	4707.93	4690.51	4915.31	4466.80
Barren	0.76	0.49	0.40	0.44	0.31	0.72
Impervious	2475.39	2758.03	3221.89	3760.15	4379.86	4915.66

Characterization of Landscape Types

One needs to analyze the change in land use types to study the change in landscape pattern index. From Table 4, it can be seen that from 2000 to 2020, the area share of each land use type in Hunan Province is forest land > cultivated land > water body > impervious surface > shrubland > grassland > bare land, with cultivated land and forest land as the main land use types, with cultivated land accounting for 33.48% of the average annual area, forest land accounting for 62.47%, and the rest of the average annual area accounting for a smaller proportion. Overall, the cropland and impervious surface area showed an increasing trend, while the rest of the land use types showed a decreasing trend, with woodland decreasing the most.

Analyzing the dynamic changes in land use types (Fig. 9) reveals that the combined land use dynamics (D_c) during the five periods were 0.19%, 0.32%, 0.07%, 0.10%, and 0.11%. This data indicates a general trend of initial increase followed by a decrease. The characteristics of single land use dynamics vary across each period. Cropland dynamics were positive from 2000 to 2012, showing an increasing trend; however, they turned negative from 2012 to 2020, with the area decreasing year by year. Forest showed negative values from 2000 to 2016, indicating a continuous decrease in area, but turned positive from 2016 to 2020, starting to show an increase. Shrubland consistently exhibited negative dynamics, experiencing a continual decrease in the area across all periods. Both grassland and water followed a similar pattern, showing positive dynamics only from 2008 to 2012 and 2012 to 2016 and negative dynamics otherwise, resulting in an overall decrease in area. Barren saw a sharp increase in 2016-2020, marked by positive dynamics, although its area as a percentage of the total remained so small that the change was negligible. Impervious consistently showed positive dynamics across all periods, continuing to increase across the total area.

Analysis of the Coupling Relationship Between 'Human-Air-Ground'

The correlation coefficient method can be used to analyze the correlation between landscape indices, and
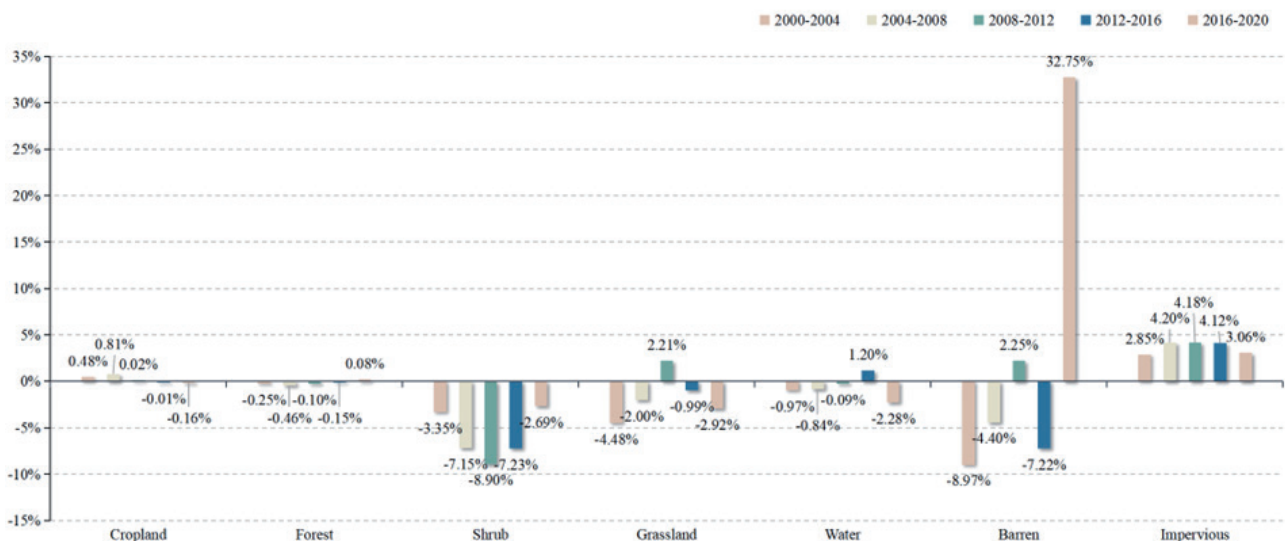

Fig. 9. Comparison of attitudes towards movement by landscape type in Hunan Province from 2000 to 2020.

the t-test is used to verify the degree of significance of the correlation relationship between landscape indices [48]. The significant degree of correlation relationship was analyzed for several landscape pattern indices selected in the previous section (Section 1.3), and the results were as follows: (1) The correlation relationship between edge density (ED) and the shape index (LSI) was stronger in significant degree, and the correlation relationship between the shape index LSI and the other indices was more pronounced: therefore, the edge density (ED) was retained. (2) The aggregation index (AI), the average patch area (AREA_MN), and cohesion (COHESION) all characterize the structural features of the landscape category, but the average patch area (AREA_MN) and cohesion (COHESION) have strong correlations with the other indices, so the cohesion index (AI) is retained; (3) The proportion of the landscape area accounted for by the patches (PLAND) and the density of patches (PD) have a strong correlation, but PD is weakly correlated with other indices and can contain more information, so PD is retained. In order to further analyze the coupling relationship between "people, air, and land", the landscape pattern indices were selected as Aggregation Index (AI), Patch Density (PD), and Edge Density (ED).

By analyzing the changes in land use types in the above (section 2.3), it can be seen that cropland and forest land, as the main land use types, have relatively obvious changes in dynamics and attitudes; water bodies and impervious surfaces come second; and the remaining types account for a very small proportion of the total and can be neglected. Therefore, we focus on analyzing the coupling relationship of 'Human-Air-Ground' among cropland, forest land, water bodies, and impervious surfaces. According to Table 5, it can be realized:

The aggregation index (AI) and edge density (ED) of cropland were positively correlated with the annual average concentration of $PM_{2.5}$ and the risk of population exposure, while the patch density (PD) was negatively correlated. Comparative analysis of the characteristics of the changes in the average annual concentration of $PM_{2.5}$ and the risk of population exposure: it was found that from 2000 to 2020, the cultivated area and the average annual concentration of $PM_{2.5}$ and the risk of population exposure showed a trend of increasing and then decreasing. This was mainly concentrated in all or part of the districts and counties of Changde, Yueyang, and Yiyang, as well as the edge of the Chang - Zhu - Tan urban agglomeration, etc., and the area with a high average annual concentration of $PM_{2.5}$ and the risk of population exposure was high and localized in the space. The autocorrelation aggregation characteristics of this region are all characterized as high - high aggregation areas. The high degree of patch aggregation, high edge density, and low fragmentation of cultivated land will lead to an increase in the annual average $PM_{2.5}$ concentration and population exposure risk. The effect of cropland on $PM_{2.5}$ annual mean concentration and

population exposure risk has a significant seasonal effect. During the growing period, the vegetation adsorption capacity can slowly stagnate the dust and reduce the $PM_{2.5}$ concentration in the air, while the bare ground and straw burning during the harvesting and planting period can produce large dust, which will increase the $PM_{2.5}$ concentration.

Edge Density (ED) and Patch Density (PD) of woodland were positively correlated with the annual mean concentration of $PM_{2.5}$ and population exposure risk, while the Aggregation Index (AI) was negatively correlated. Comparative analysis of the characteristics of changes in the mean annual concentration of $PM_{2.5}$ and population exposure risk: it was found that the area of forest land showed a decreasing and then increasing trend in relation to the mean annual concentration of $PM_{2.5}$ and population exposure risk, which was mainly concentrated in all or part of the counties and districts of Yongzhou, Chenzhou, Huaihua, and Shaoyang. The low mean annual concentration of $PM_{2.5}$, the low population exposure risk, and the autocorrelation aggregation characteristics of the local space are manifested in the low - low aggregation area. The high degree of patch aggregation, low edge density, and low degree of fragmentation of woodland are conducive to reducing annual average $PM_{2.5}$ concentration and population exposure risk. The main reason why woodland can effectively reduce $PM_{2.5}$ concentration is that concentrated and complex-shaped plant leaves can adsorb and immobilize particulate matter, reduce atmospheric particulate matter concentration, lower the risk of population exposure to $PM_{2.5}$, and improve air quality.

The Aggregation Index (AI), Edge Density (ED), and Patch Density (PD) of water bodies and impervious surfaces were all positively correlated with the annual average concentration of $PM_{2.5}$ and population exposure risk. Comparative analysis of the characteristics of changes in the annual average concentration of $PM_{2.5}$ and population exposure risk finds that the area of water bodies decreased year by year, the area of impervious surfaces increased year by year, and both of them were mainly concentrated in all or part of the districts and counties of Changde, Yueyang, and Yiyang and the center of the Chang - Zhu - Tan urban agglomeration. The region with a high annual average concentration of $PM_{2.5}$ and a high risk of population exposure and the characteristics of the local spatial autocorrelation aggregation were all manifested as a high - high aggregation area. Higher aggregation of water bodies and impervious surfaces, higher density of edges, and more complex fragmentation result in higher annual average $PM_{2.5}$ concentration and population exposure risk. Therefore, the increase of impervious surfaces and the decrease of water bodies will increase the risk of $PM_{2.5}$ annual average concentration and population exposure, and the reasonable control of impervious surfaces extension edge zone and fragmentation degree

Table. 5. Correlation coefficients of the coupling relationship between 'Human-Air-Ground'.

Landscape Type	Landscape pattern index	PM$_{2.5}$ Annual Average Concentration						PM$_{2.5}$ Population Exposure Risk PM$_{2.5}$					
		2000	2004	2008	2012	2016	2020	2000	2004	2008	2012	2016	2020
Cropland	AI	0.712**	0.766**	0.713**	0.701**	0.735**	0.762**	0.731**	0.725**	0.717**	0.710**	0.707**	0.705**
	ED	0.449**	0.508**	0.431**	0.413**	0.446**	0.456**	0.677**	0.665**	0.614**	0.627**	0.658**	0.656**
	PD	-0.378**	-0.458**	-0.400**	-0.422**	-0.495**	-0.533**	-0.342**	-0.378**	-0.368**	-0.379**	-0.434**	-0.430**
Forest	AI	-0.810**	-0.855**	-0.805**	-0.782**	-0.825**	-0.861**	-0.832**	-0.834**	-0.845**	-0.850**	-0.856**	-0.867**
	ED	0.189*	0.172	0.100	0.069	0.069	0.070	0.358**	0.293**	0.198*	0.167	0.175	0.197*
	PD	0.528**	0.565**	0.475**	0.464**	0.524**	0.577**	0.677**	0.666**	0.639**	0.640**	0.664**	0.680**
Shrubland	AI	-0.551**	-0.598**	-0.653**	-0.587**	-0.568**	-0.493**	-0.527**	-0.484**	-0.571**	-0.479**	-0.445**	-0.395**
	ED	-0.757**	-0.810**	-0.783**	-0.748**	-0.779**	-0.717**	-0.730**	-0.720**	-0.713**	-0.667**	-0.667**	-0.628**
	PD	-0.764**	-0.817**	-0.786**	-0.756**	-0.778**	-0.742**	-0.738**	-0.729**	-0.714**	-0.671**	-0.677**	-0.654**
Grassland	AI	-0.466**	-0.363**	-0.356**	-0.459**	-0.240**	-0.286**	-0.395**	-0.312**	-0.242**	-0.375**	-0.208*	-0.236**
	ED	-0.530**	-0.494**	-0.445**	-0.467**	-0.436**	-0.433**	-0.469**	-0.313**	-0.230*	-0.296**	-0.323**	-0.315**
	PD	-0.537**	-0.526**	-0.490**	-0.479**	-0.535**	-0.488**	-0.452**	-0.331**	-0.266**	-0.281**	-0.394**	-0.368**
Water	AI	0.228*	0.224*	0.231*	0.300**	0.316**	0.244**	-0.011	0.010	0.005	0.071	0.112	0.083
	ED	0.695**	0.680**	0.656**	0.638**	0.646**	0.645**	0.491**	0.444**	0.434**	0.425**	0.408**	0.403**
	PD	0.688**	0.704**	0.661**	0.620**	0.639**	0.622**	0.595**	0.548**	0.545**	0.530**	0.502**	0.446**
Barren	AI	0.045	0.014	0.019	0.022	-	-	-0.032	-0.037	-0.030	-0.027	-	-
	ED	0.063	0.001	0.002	0.099	0.090	0.097	0.014	0.014	-0.029	0.131	0.134	0.135
	PD	0.063	0.001	0.002	0.099	0.090	0.098	0.014	0.014	-0.029	0.130	0.133	0.136
Impervious	AI	0.204*	0.081	0.186*	0.232*	0.204*	0.171	0.050	0.056	0.130	0.198*	0.204*	0.209*
	ED	0.439**	0.574**	0.486**	0.450**	0.522**	0.599**	0.738**	0.774**	0.762**	0.767**	0.791**	0.808**
	PD	0.364**	0.538**	0.404**	0.337**	0.426**	0.519**	0.678**	0.721**	0.685**	0.671**	0.692**	0.706**

Note: * and ** are significant correlations at the 0.05 and 0.01 levels (two-tailed), respectively.

can effectively mitigate $PM_{2.5}$ pollution and reduce the risk of population exposure.

Characterization of the Spatial and Temporal Evolution of the Risk of $PM_{2.5}$ Population Exposure

In the context of green development, sustainable development is the top priority of urban construction. $PM_{2.5}$, as an important indicator of urban green development, is closely related to industrial production, industrial structure, and road transportation networks. The author takes the spatial and temporal distribution characteristics of $PM_{2.5}$ annual average concentration and population exposure risk as an entry point to analyze the correlation between the landscape pattern index and $PM_{2.5}$ annual average concentration and population exposure risk. The annual average concentration of $PM_{2.5}$ in Hunan Province from 2000 to 2020 has been slowly increasing and then significantly decreasing, and the year 2013 is the turning point of the decrease, which is mainly caused by two aspects: first, the 2012 Eighteenth National Congress of the Party of China (CPC) set a new target to increase the annual average concentration of $PM_{2.5}$ in Hunan Province, and the second one is to decrease the average concentration in Hunan Province. First, the 18th Party Congress in 2012 listed "ecological civilization construction" for the first time in the overall layout of the socialist cause with Chinese characteristics and launched various strategic deployments for ecological civilization construction. Second, the Action Plan for Prevention and Control of Air Pollution issued by the State Council in 2013 clearly stated that practical and effective measures should be taken to strengthen ecological civilization construction and optimize industrial structure to alleviate the atmospheric environmental problems with $PM_{2.5}$ as the characteristic pollutant. The spatial distribution is high in the northeast and low in the southwest. The high-value area is concentrated in the Chang - Zhu - Tan area, with rapid economic development and a high urbanization level, which indicates that $PM_{2.5}$ is closely related to economic development, industrial structure, and industrial energy. The spatial distribution characteristics of the annual average concentration of $PM_{2.5}$ and the risk of exposure of the population have consistency, with a significant positive autocorrelation in the global space and obvious clustering characteristics in the local area. The high-value area and the low-value area of both of them coincide spatially, which is in agreement with the spatial distribution of $PM_{2.5}$, spatially coinciding, which is consistent with the findings of Fu [49]. The high urbanization level, large population base, and rapid industrial development in the high-value area all lead to an increase in $PM_{2.5}$ emissions, exposing the population to a high-risk area for a long time, while the low-value area has a complex hilly terrain, a high vegetation cover, a small population base, a slow industrialization development, and low socio-economic

energy consumption, which results in a low level of risk of population exposure to $PM_{2.5}$.

Analysis of the Association Between Different Types of Landscape Patterns and the Risk of Population Exposure to $PM_{2.5}$

The landscape pattern index is a quantitative index reflecting the spatiotemporal heterogeneity of the landscape, which can accurately extract the characteristics of the landscape pattern and is currently the most direct and effective research method in the analysis of spatiotemporal dynamics of the landscape pattern [50]. Using the optimal moving window method to explore the correlation between landscape patterns and annual average $PM_{2.5}$ concentration and population exposure risk can improve the scientific validity of the research results. A large number of studies have shown [51, 52] that different land use types have a significant effect on $PM_{2.5}$ concentration, and changes in landscape type are correlated with population exposure risk to a certain extent. By analyzing the dynamic attitude of land use, it was found that the strength of the correlation of the landscape pattern index was consistent with the corresponding single dynamic attitude change, indicating that the degree of change in land use type has an impact on the landscape pattern, which in turn affects the annual average $PM_{2.5}$ concentration and population exposure risk [53]. Similar to the results of other studies, landscape types such as woodland, shrubs, and grassland were negatively correlated with annual mean $PM_{2.5}$ concentrations, mainly attributed to green plants' ability to effectively adsorb particulate matter in the air, thereby reducing air pollution. Cultivated land, on the other hand, showed a positive correlation with $PM_{2.5}$ concentration, contrary to some studies' results [54]. Among them, related scholars found that arable land has a "source" and "sink" phenomenon on $PM_{2.5}$ concentration, not only as a type of vegetation cover adsorption of stagnant dust but also in the harvesting and sowing seasons due to the surface of the bare dust. The results of the present study confirm that arable land is more likely to exacerbate the $PM_{2.5}$ concentration of the air and is likely to exacerbate $PM_{2.5}$ air pollution. The positive correlation between the landscape pattern index of water bodies and $PM_{2.5}$ is different from the results of some studies [55], while the present study confirms that water bodies act as a long time series of pollutant retention, which leads to high air pollutant concentration levels around the water bodies in the form of pollutant sources. Regional economic development, urbanization, and industrialization have increased the complexity and fragmentation of bare land and impervious surface land patches, leading to higher annual average concentrations of $PM_{2.5}$. HART R [56] and BENCHRIF A [57] assessed that population exposure risk is closely related to the human habitat and that environmental risk assessment is important for improving urban construction and social equity. Like the $PM_{2.5}$ correlation, the landscape

index of woodland, shrub, and grassland green space sites showed a significant negative correlation with population exposure risk. Overall, the correlation between impervious surface and exposure index was greater than that of other sites, indicating that the impact of urban construction is stronger than other factors [58].

Conclusions

In this paper, the landscape pattern index, annual average $PM_{2.5}$ concentrations, and population exposure risk of different land use types at the fine grid scale in Hunan Province are studied. The population exposure risk model, moving window method, spatial autocorrelation model, and correlation analysis are used to explore the spatial and temporal evolution characteristics of annual average $PM_{2.5}$ concentration and population exposure risk from 2000 to 2020. It reveals the characteristics of the spatial and temporal evolution of the "people-air-land" coupling relationship and its spatial heterogeneity in the study area. The spatial and temporal evolution characteristics of the coupling relationship between 'Human-Air-Ground' and its spatial heterogeneity were revealed. The results show that:

(1) From 2000 to 2020, the annual average concentration of $PM_{2.5}$ in Hunan Province as a whole shows a slow increase and then a significant decrease; the spatial distribution is high in the northeast and low in the southwest, and the high-value areas ($PM_{2.5}$ > 45 $\mu g/m^3$) are mainly located in Changsha, Xiangtan, Zhuzhou, Changde, Yueyang, Yiyang, and so on. This is a high - high agglomeration area located in the center of the urban agglomeration's economic development, with flat terrain and concentrated cities where human activities are active. It is located in the center of the economic development of urban agglomerations, with flat terrain and concentrated cities, active human activities, and aggregation of $PM_{2.5}$ air pollutants. The low - low aggregation zone is mainly distributed in all or part of districts and counties, such as Yongzhou, Chenzhou, Huaihua, and Shaoyang, which are relatively backward in terms of socio-economics and forested with mountainous hills, with high vegetation coverage and superior ecological environment, which is conducive to the deposition and absorption of $PM_{2.5}$ pollutants.

(2) From 2000 to 2016, Hunan Province was exposed to $PM_{2.5}$ annual average high concentration areas (>45 $\mu g/m^3$), accounting for 74.24% of the average value. From 2016 to 2020, the proportion of the population in the areas exposed to $PM_{2.5}$ annual average low concentration values (<35 $\mu g/m^3$) increased year by year, from 6.86% to 73.02%. In particular, 2020 appeared to be when the $PM_{2.5}$ population share of areas with annual average concentrations in the range of 15-25 $\mu g/m^3$ is 13.2%, and there are no areas above 45 $\mu g/m^3$. The risk of $PM_{2.5}$ population exposure in the spatial distribution is dominated by low risk, accounting for more than 70% of the total area, which is mainly dispersed in the fringe cities and districts and counties in Hunan Province, as a low - low aggregation area, which is related to its location in the mountainous and hilly areas, high vegetation coverage, small population size, slow industrialization, low socio-economic energy consumption, and low pollution emissions. The high-risk areas are mainly concentrated in the Chang - Zhu - Tan urban agglomeration center. The region has a scattered heterogeneous distribution, has a high - high aggregation area, is the root of urbanization and industrialization development, and has led to the growth of $PM_{2.5}$ emissions so that the population is exposed to a high concentration range for a long time.

(3) Cultivated land and forested land, as the main land types in Hunan Province, are characterized by relatively obvious changes in dynamics and attitudes; water bodies and impervious surfaces are the second most common; therefore, we focused on analyzing the correlation between the landscape pattern indices of cultivated land, forested land, water bodies, and impervious surfaces and the risk of population exposure to the annual average $PM_{2.5}$ concentration and population exposure. Among them, a high degree of patch aggregation, high edge density, and low degree of fragmentation of cropland led to higher annual mean $PM_{2.5}$ concentration and population exposure risk, and the correlations of patch aggregation and edge density were stronger than those of fragmentation. Higher levels of patch aggregation, lower edge densities, and lower levels of fragmentation in woodlands contribute to lower $PM_{2.5}$ annual mean concentrations and population exposure risk, and the levels of patch aggregation and fragmentation are more strongly correlated than edge densities. Higher aggregation, higher edge density, and more complex fragmentation of water bodies and impervious surfaces resulted in a higher risk of $PM_{2.5}$ annual mean concentrations and population exposure, and edge density and fragmentation were more closely correlated than patch aggregation.

Acknowledgments

Conflicts of Interest

The authors declare no conflicts of interest.

References

1. GUO W.W., CHEN Y.J., LIU G., SONG K.S., TAO B.X. Analysis on the characteristics and influencing factors of air quality of urban agglomeration in the middle reaches of the Yangtze River in 2016 to 2019. Ecology and Environmental Sciences, **29** (10), 2034, **2020**.

2. XU W.J., ZENG Z.T., XU Z.Y., LI X.D., CHEN X.W., LI X., XIAO R., LIANG J., CHEN G.J., LIN A.Q., LI J.J., ZENG G.M. Public health benefits of optimizing urban industrial land layout-The case of Changsha, China. Environmental Pollution, **263**, 114388, **2020**.

3. ZHANG Y.N., PAN J.H. Spatiotemporal simulation and differentiation pattern of carbon emissions in China based on DMSP/OLS nighttime light data. China Environmental Science, **39** (4), 1436, **2019**.

4. ZHANG M.M., TAN S.K., LIANG J.S., ZHANG C., CHEN E.Q. Predicting the impacts of urban development on urban thermal environment using machine learning algorithms in Nanjing, China. Journal of Environmental Management, **356**, 120560, **2024**.

5. CHEN W.Q., RAN H.F., CAO X.Y., WANG J.Z., TENG D.X., CHEN J., ZHENG X. Estimating $PM_{2.5}$ with high-resolution 1-km AOD data and an improved machine learning model over Shenzhen, China. Science of the Total Environment, **746**, 141093, **2020**.

6. LI Y., XIAO L.M., HU W.M., YI M., XIE Y.Z. Spatio-temporal pattern of land use change in Changsha-Zhuzhou-Xiangtan Core Areas and its driving forces. Economic Geography, **41** (7), 173, **2021**.

7. WAN Q., CHEN Z., WANG Y., FENG B. Spatiotemporal Evolution of $PM_{2.5}$ in the Yangtze River Economic Belt during 1998-2016 by Multiscale Analysis. Resources and Environment in the Yangtze Basin, **28** (10), 2504, **2019**.

8. HOU S.X., ZHANG J.D., LI J. Analysis of spatiotemporal distribution and correlation factors of atmospheric pollutants in Shanghai city. Ecology and Environmental Sciences, **30** (6), 1220, **2021**.

9. WANG J.Y., WANG S.J., LI S.J. Examining the spatially varying effects of factors on $PM_{2.5}$ concentrations in Chinese cities using geographically weighted regression modeling. Environmental Pollution, **248**, 792, **2019**.

10. GUO Y., JIANG Y.D., HUANG B.Z., XING J.J., WEI Z.Z. Health Impact of $PM_{2.5}$ and O3 and Forecasts for Next 10 Years in China. Research of Environmental Sciences, **34** (4), 1023, **2021**.

11. REIS S., LISKA T., VIENO M., CARNELL E.J., BECK R., CLEMENS T., DRAGOSITS U., TOMLINSON S.J., LEAVER D., HEAL M.R. The influence of residential and workday population mobility on exposure to air pollution in the UK. Environment International, **121**, 803, **2018**.

12. ABDULAZIZ M., ALSHEHRI A., BADRI H., SUMMAN A., SAYQAL A. Concentration Level and Health Risk Assessment of Heavy Metals in $PM_{2.5}$ in Ambient Air of Makkah City, Saudi Arabia. Polish Journal of Environmental Studies, **31** (5), 3991, **2022**.

13. ZHANG X.Y., HU H.B. Risk Assessment of Exposure to $PM_{2.5}$ in Beijing Using Multi-Source Data. Acta Scientiarum Naturalium Universitatis Pekinensis, **54** (5), 1103, **2018**.

14. ZHANG M.M., CHEN E.Q., ZHANG C., LIU C., LI J.X. Multi-Scenario Simulation of Land Use Change and Ecosystem Service Value Based on the Markov–FLUS Model in Ezhou City, China. Sustainability, **16**, 6237, **2024**.

15. LI Y.X., WANG C.X., LIU Y.X. Multi-objective optimization of land use based on ecosystem service bundle zoning: A case study of Bayannur City. Chinese Journal of Ecology, **42** (5), 1205, **2023**.

16. XIAO J.Y., HE C., MU H., YANG L., HUANG J.Y., XIN A.X., TU P.Y., HONG S. Spatiotemporal pattern and population exposure risks of air pollution in Chinese urban areas. Progress in Geography, **40** (10), 1650, **2021**.

17. MI K.N., ZHUANG R.L., LIANG L.W., DUAN Y.P., GAO J. Spatiotemporal evolution and characteristics of $PM_{2.5}$ in the Yangtze River Delta based on real-time monitoring data during 2013-2016. Geographical Research, **37** (8), 1641, **2018**.

18. LIAO L.X. CHEN J. Study on the Spatiotemporal Characteristics and Influencing Factors of Population Exposure to Particulate Matter $PM_{2.5}$ in Henan Province. Journal of Fujian Normal University (Natural Science Edition), **38** (1), 59, **2022**.

19. LIN J.H., CHEN W.H., ZHANG A. Analysis of $PM_{2.5}$ population exposure doses characteristics in Beijing in 2019. Journal of Geo-information Science, **22** (12), 2348, **2020**.

20. MU H., HE C., RUAN Q.M., WANG D.L., ZHOU X.Y., YANG L., TU P.Y., WANG H.J., HONG S. Spatiotemporal distribution characteristics and population exposure risks to $PM_{2.5}$ in countries along the Belt and Road. Acta Scientiae Circumstantiae, **41** (6), 2229, **2021**.

21. TANG P.C. Study on temporal and spatial evolution and influencing factors of $PM_{2.5}$ population exposure risk in Anhui Province. Hefei University, **2022**.

22. TONG L.G., LI X.M., HUANG Z., ZHANG J., TIAN S.Z. Study on risk of population exposure to $PM_{2.5}$ in Baotou City. Journal of Arid Land Resources and Environment, **31** (11), 50, **2017**.

23. XU D., LIN W.P., SHI R.H., GAO J., LI L.B. Spatial-temporal evolution patterns of $PM_{2.5}$ exposure risk in the Yangtze River Delta Ecological Greening Development Demonstration Area during 2001-2020. Acta Scientiae Circumstantiae, **42** (8), 36, **2022**.

24. ZHANG L.L., PAN J.H. Spatial-temporal pattern of population exposure risk to $PM_{2.5}$ in China. China Environmental Science, **40** (1), 1, **2020**.

25. CHEN M.X., GUO S.S., HU M.G., ZHANG X.P. The spatiotemporal evolution of population exposure to $PM_{2.5}$ within the Beijing-Tianjin-Hebei urban agglomeration, China. Journal of Cleaner Production, **265**, 121708, **2020**.

26. SINGH V., SOKHI R.S., KUKKONEN J. An approach to predict population exposure to ambient air $PM_{2.5}$ concentrations and its dependence on population activity for the megacity London. Environmental Pollution, **257**, 113623, **2020**.

27. LIM A., OWUSU B.A., THONGROD T., KHURRAM H., PONGSIRI N., INGVIYA T., BUYA S. Trend and Association Between Particulate Matters and Meteorological Factors: A Prospect for Prediction of $PM_{2.5}$ in Southern Thailand. Polish Journal of Environmental Studies, **2024**.

28. SHARMA D., SAPAN T., DEEPTY J., KAMNA S. Mapping the Spatiotemporal Variability of Particulate Matter Pollution in Delhi: Insights from Land Use Regression Modelling. Journal of the Indian Society of Remote Sensing, **52,** 1329, **2024.**

29. GHESHLAGHPOOR S., ABEDI S.S., MOGHBEL M. The relationship between spatial patterns of urban land uses and air pollutants in the Tehran metropolis, Iran. Landscape Ecology, **38**, 553, **2023**.

30. MENGISTE B.M., SHI W., WONG M.S. Urban landscape and development effects on city sustainability: a systematic review of empirical studies. Environment, Development and Sustainability, **2024**.

31. MCCARTY J., KAZA N. Urban form and air quality in the United States. Landscape and Urban Planning, **139**, 168, **2015**.

32. ZOU B., PENG F., JIAO L.M., WENG M. GIS Aided Spatial Zoning of High-Resolution Population Exposure to Air Pollution. Geomatics and Information Science of Wuhan University, **38** (3), 334, **2013**.

33. GUO J.B., ZHANG Y., HANG Z.W., HOU L., ZENG W.L. Land use change and its driving mechanism in the alpine gorge of southeast Tibet based on geodetector: A case study of Nyingchi City. Journal of China Agricultural University, **28** (4), 210, **2023**.

34. CAI L.Y., ZHUANG M.Z., REN Y. A landscape scale study in Southeast China investigating the effects of varied green space types on atmospheric $PM_{2.5}$ in mid-winter. Urban Forestry & Urban Greening, **49**, 126, **2020**.

35. WU Z.J., LI Z.J., ZENG H. A gradient analysis of urban landscape pattern in Huizhou. Chinese Journal of Ecology, **40** (2), 490, **2021**.

36. ZHANG M.M., İLKER Y., FAITH A., HU C.G., CHEN E.Q., AHMET E.S., NECMETTIN E., MUSTAFA U., AŞIR Y.K. Impact of Urban Surfaces on Microclimatic Conditions and Thermal Comfort in Burdur, Türkiye. Atmosphere, **15** (11), 1375, **2024**.

37. ZHANG M.M., TAN S.K., CHEN E.Q., LI J.X. Spatio-temporal characteristics and influencing factors of land disputes in China: Do socio-economic factors matter? Ecological Indicators, **160**, 111938, **2024**.

38. WANG Z.Q, JIANG S., XU S., ZHANG J.X., MUMTAZ F., ZHANG M. Spatial patterns and its influencing factors on villages around the Ji-shape bend of the Yellow River. Frontiers in Environmental Science, **12**, 1477693, **2024.**

39. LI W.X., YAN Z.G. Analysis of spatiotemporal evolution of land use and its driving mechanism in the agro-pastoral ecotone of Gansu Province using Geodetector. Arid Zone Research, **41** (4), 590, **2024**.

40. ZHANG M.M., TAN S.K., PAN Z.C., HAO D.Q., ZHANG X.S., CHEN Z.H. The spatial spillover effect and nonlinear relationship analysis between land resource misallocation and environmental pollution: Evidence from China. Journal of Environmental Management, **321**, 115873, **2022**.

41. WANG A., ZHANG M.M., CHEN E.Q., ZHANG C., HAN Y.J. Impact of seasonal global land surface temperature (LST) change on gross primary production (GPP) in the early 21st century, Sustainable Cities and Society, **110**, 105572, **2024**.

42. RINCON G., MORANTES G., ROA-LOPEZ H., CORNEJO-RODRIGUEZ M.D.P., JONES B., CREMADES L.V. Spatio-temporal statistical analysis of PM1 and $PM_{2.5}$ concentrations and their key influencing factors at Guayaquil city, Ecuador. Stochastic Environmental Research and Risk Assessment, **37**, 1093, **2023**.

43. KARIMI B., SHOKRINEZHAD B. Spatial variation of ambient $PM_{2.5}$ and PM10 in the industrial city of Arak, Iran: A land-use regression. Atmospheric Pollution Research, **12** (12), 101235, **2021**.

44. YANG J., HUANG X. The 30 m annual land cover dataset and its dynamics in China from 1990 to 2019. Earth System Science Data, **13** (8), 3907, **2021**.

45. GOU A.P., LI W.X., WANG J.B. Spatiotemporal Correlation Between Green Space Landscape Pattern and $PM_{2.5}$ Concentration in Chongqing City, China. Journal of Earth Sciences and Environment, **46** (1), 25, **2024**.

46. YANG K., ZHOU Z.X., BAI J.Z., LIU H.W. Effect of landscape pattern index on $PM_{2.5}$ simulation in Guanzhong Plain Urban Agglomeration. Journal of Shanxi Normal University (Natural Science Edition), **50** (4), 115, **2022**.

47. FENG Y.F., FENG J.M., LI C. Progress of the spatiotemporal change and improvement green space from the perspective of ecological resilience. Acta Ecologica Sinica, **43** (14), 5648, **2023**.

48. SUN Y.X. Study on Accessibility to Urban Green Space based on Road Distance and Its Equity. University of Chinese Academy of Sciences, Beijing, **2018**.

49. FU J.H., ZHOU F.Z. Chinese provincial air quality measurement and its influencing factors. Urban Problems, (5), 20, **2020**.

50. LU Z.D., ZHANG M.M., HU C.G., MA L.L., CHEB E.Q., ZHANG C., XIA G.Z. Spatiotemporal Changes and Influencing Factors of the Coupled Production–Living–Ecological Functions in the Yellow River Basin, China. Land, **13**, 1909, **2024**.

51. ŁOWICKI D. Landscape pattern as an indicator of urban air pollution of particulate matter in Poland. Ecological Indicators, **97**, 17, **2019**.

52. ZARIN T., ESRAZ-UL-ZANNAT M. Assessing the potential impacts of LULC change on urban air quality in Dhaka city. Ecological Indicators, **154**, 110746, **2023**.

53. CHEN X.J., ZHANG J.T., ZHANG C.C, PENG X.J. Spatial and Temporal Variation of $PM_{2.5}$ Concentrations Based on Thiesen Polygon and its Correlation with Land-use Patterns in Nanjing City. Bulletin of Soil and Water Conservation, **38** (1), 293, **2018**.

54. NIU X., LI Y., LI M.N., ZHANG T., MENG H., ZHANG Z., WANG B., ZHANG W.K. Understanding vegetation structures in green spaces to regulate atmospheric particulate matter and negative air ions. Atmospheric Pollution Research, **13** (9), 101534, **2022**.

55. FAN Z.Y., ZHAN Q.M., LIU H.M., XIA Y. Investigating the interactive and heterogeneous effects of green and blue space on urban $PM_{2.5}$ concentration, a case study of Wuhan. Journal of Cleaner Production, **378**, 134389, **2022**.

56. HART R., LIANG L., DONG P. Monitoring, Mapping, and Modeling Spatial–Temporal Patterns of $PM_{2.5}$ for Improved Understanding of Air Pollution Dynamics Using Portable Sensing Technologies. International Journal of Environmental Research and Public Health, **17** (14), 4914, **2019**.

57. BENCHRIF A., WHEIDA A., TAHRI M., SHUBBAR R.M., BISWAS B. Air quality during three covid-19 lockdown phases: AQI, $PM_{2.5}$ and NO_2 assessment in cities with more than 1 million inhabitants. Sustainable Cities and Society, **74**, 103170, **2021**.

58. ZHANG H., LI C.S., ZENG X.J. Study on the Correlation Relationship Between Land Use Structure and Air Quality Based on Spatial Econometric Models: A Case Study of Cities and Countiesin Guangdong, Fujian and Zhejiang Provinces. Modern Urban Research, **39** (2), 9, **2024**.